SPE-183929-MS

Processing Frequent 4D Land Seismic Data with Buried Sensors for CO_2 Monitoring

Abdullah Al Ramadhan, Emad Hemyari, Andrey Bakulin, Kevin Erickson, Robert Smith, and Michael A. Jervis, EXPEC Advanced Research Center, Saudi Aramco

Copyright 2017, Society of Petroleum Engineers

This paper was prepared for presentation at the SPE Middle East Oil & Gas Show and Conference held in Manama, Kingdom of Bahrain, 6-9 March 2017.

This paper was selected for presentation by an SPE program committee following review of information contained in an abstract submitted by the author(s). Contents of the paper have not been reviewed by the Society of Petroleum Engineers and are subject to correction by the author(s). The material does not necessarily reflect any position of the Society of Petroleum Engineers, its officers, or members. Electronic reproduction, distribution, or storage of any part of this paper without the written consent of the Society of Petroleum Engineers is prohibited. Permission to reproduce in print is restricted to an abstract of not more than 300 words; illustrations may not be copied. The abstract must contain conspicuous acknowledgment of SPE copyright.

Abstract

In 2015, Saudi Aramco started a CO_2 Water-Alternating-Gas (WAG) EOR pilot project in an onshore carbonate reservoir. To monitor lateral expansion of the CO_2 plume, the area was instrumented with a hybrid surface/downhole permanent seismic monitoring system. This system consists of over 1000 buried seismic sensors at a depth of around 70 m, below the the depth of expected weathering layer to mitigate the time-lapse noise. Despite receiver burial, seismic data still suffers from numerous challenges including: significant amounts of high-amplitude coherent noise such as guided waves, mode conversions, and scattered energy; amplitude variations over space and time caused by source and receiver coupling; variability of wavelet shape and arrival times due to seasonal near-surface variations; and low signal-to-noise ratio (SNR). A novel processing workflow was designed for 4D processing of such data. The workflow involves five critical processes. First, the high-amplitude coherent noise is eliminated using FK-based techniques that are 4D compliant to preserve the reservoir changes between repeated seismic surveys. Second, a four-term joint surface-consistent amplitude-scaling algorithm resolves the amplitude variations. The algorithm allows both source and receiver terms to have different scalars for the same positions, but it restricts the other two terms to be position-invariant over different time-lapse surveys, as the window of analysis does not include the reservoir. This is to guarantee that the source and receiver terms are survey-dependent while the other two terms are survey-independent. Thus, the amplitude variability is linked to source and receiver positions over space and time. It also assures that the reservoir changes are not affected by changes in the overburden. Third, wavelet shape variations are addressed using a four-term joint surface-consistent spiking deconvolution algorithm that applies similar principle as the scaling algorithm. Fourth, the small variations in reflection times between different surveys (4D statics) caused by seasonal variations are corrected by a specialized surface-consistent residual statics algorithm using a common pilot derived from the base survey. Fifth, the pre-stack data is supergrouped to enhance the signal-to-noise ratio and repeatability.

The processing workflow has been applied to frequent land 3D seismic data acquired over a CO_2 WAG EOR pilot project in Saudi Arabia. As a result, we obtained very repeatable seismic images that may successfully detect small CO2-related changes in a stiff carbonate reservoir.

Introduction

Petroleum reservoir complexity is a function of heterogeneities in the reservoir properties, which has a direct impact on hydrocarbon recovery. The current practice of 3D surface seismic and well testing data cannot confidently identify the spatial variability of the flow-controlling properties within the reservoir due to lack of sufficient details. Therefore, it may be best achieved by time-lapse seismic method. Time-lapse seismic, also known as 4D seismic, has attracted an increasing attention as a technology for monitoring and managing petroleum reservoirs injected with CO_2 at many sites (Davis et al., 2003; Li, 2003; Maldal and Tappel, 2004; Torp and Gale, 2004; White et al., 2004; Mathieson et al., 2010; Urosevic et al., 2010; Eiken et al., 2011; Pevzner et al., 2011; Arts et al., 2013; Ringrose et al., 2013). The reason for this increase is the attractive features that could lead to a better understanding of the complex nature of petroleum reservoirs, the production properties, and composition. The practice of the method consists of conducting repeated 3D seismic surveys at different time intervals (Lumley, 2001), separated by months or even years, over the same site, preferably with the same acquisition geometries (Meunier et al., 2001). Following the acquisition, the repeated 3D seismic surveys go through a processing workflow to reduce the noise level and thus improve the repeatability (White et al., 2015). Subsequently, the first 3D seismic survey (baseline survey) is subtracted from the repeat 3D seismic volumes (monitor surveys) to delineate the CO_2 zones by locating the changes within the petroleum reservoir. Production activities within a petroleum reservoir, such as extracting oil or injecting fluid, may result in significant changes in elastic properties that, in turn, induce variations in the seismic signal. To improve the 4D seismic technique's ability to detect the dynamic changes (4D signal) caused by the injected CO_2 within the petroleum reservoir, the noise level between the base survey and the monitor surveys has to be reduced much below the 4D signal level (Lumley et al., 2003; Bakulin et al., 2007; Schissele et al., 2009). Such a noise reduction can be achieved during both the 4D seismic acquisition and processing stages (Rickett and Lumley, 2001; Bakulin et al., 2007; Ma et al., 2009).

There are three main time-lapse processing approaches, according to the processing objective. These are the independent, the simultaneous, and the joint processing workflow (Roach et al., 2015). Furthermore, each processing workflow involves steps applied either pre-stack or post-stack. When the objective of the time-lapse processing is to optimize for repeatability, the independent approach becomes irrelevant. Clearly, the approach commonly used for time-lapse processing is a combination of simultaneous and joint processing (Meadows and Cole, 2013). Still, the simultaneous processing workflow can be used alone for time-lapse seismic datasets to improve repeatability (Li et al., 2012); however, it may be inferior to the joint processing approach (Meadows and Cole, 2013).

In order to measure repeatability and evaluate the effectiveness of the 4D seismic method over a land carbonate petroleum reservoir in the eastern province of Saudi Arabia, a combined processing workflow is applied to two repeated 3D seismic surveys, separated by a three-month time interval. The two volumes were acquired using permanent buried sensors. The processing workflow is optimized primarily for repeatability and secondarily for imaging.

Seismic monitoring project

In July 2015, Saudi Aramco commenced its first CO_2 -EOR pilot project for a land carbonate petroleum reservoir located in the Eastern Province of Saudi Arabia. The objective of the project is to monitor the expansion of the CO_2 plume over the petroleum reservoir by continuously acquiring 3D seismic data on a monthly basis. The project site imposes several geophysical challenges to the success of the project. First, the highly complex and changing near-surface hinders both imaging and data repeatability. Second, the strong noise generated by karsts and thick sand dunes obscure reflection events, while dune migration and seasonal variations lead to a non-repeatability between subsequent 3D seismic surveys. Furthermore, low level of 4D signal is predicted due to injection of CO_2 in a stiff carbonate reservoir.

To alleviate the above-mentioned problems, a dedicated hybrid system comprising of 1003 sensors and over 100,000 surface shot points is deployed as shown in Figure 1. The receivers are buried at a depth of 50-80 meters on a sparse grid of 50 by 50 m to avoid the noisy surface environment, the surface variability, and the effects of the strongly attenuating near-surface layers. This, in turn, leads to reduction in the noise level. Burying the sensors guarantees that the receiver position coordinates are perfectly repeatable over the entire project life. Vibroseis are used as seismic sources with a dense grid of 10 by 10 m. The dense grid of the sources assures that the wavefield is adequately sampled within the common-receiver gather. Based on the recorded data, the acquisition system is highly repeatable and hence contributes to the monitoring project success. The acquisition geometry layout produces a 5 by 5 m CDP bin with a nominal fold of approximately 900.

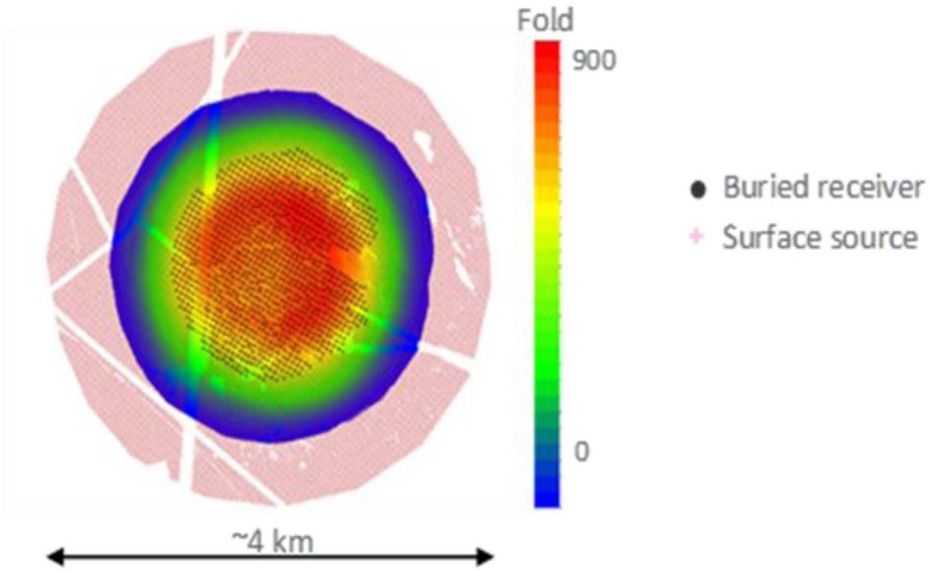

Figure 1—Geometry of the hybrid acquisition system used for CO_2 monitoring. 1003 sensors are buried at a depth between 50-80 m below the surface on a 50 by 50 m grid. Vibroseis sources on a dense grid of 10 by 10 m are deployed to safeguard high fold data, to improve SNR, and to adequately sample the wavefield.

Seismic processing workflow

The field acquisition started along with the injection in 2015 and proceeded on a continuous basis. It takes on average one month to complete a 3D seismic survey consisting of over 100,000 shots. To measure repeatability and to evaluate the effectiveness of the 4D seismic method, two repeated 3D seismic surveys, acquired using permanent buried sensors and separated by a three-month time interval, are selected for this study. The permanent buried receiver array safeguards the repeatability of sensor position but not necessarily the response over the life of the project. At the start of the CO_2 injection-monitoring project, 1003 receivers were installed, of which 27 have been excluded from processing due to sensor failure or poor coupling/ringiness. Such receivers must be removed from both baseline and monitor surveys as the primary goal of the processing is to improve repeatability. Furthermore, one must not assume uniform receiver coupling in space and time because of the burial. Shots need more careful attention to ensure that shot positions over space and time maintain their prescribed accuracy and precision. Those shot positions that violate the accuracy condition over space and/or time must be edited from the two surveys. So far, the repeated shot positions precision obtained is on average around 0.3 m from the baseline shot positions.

The primary objective of the processing workflow is to optimize for time-lapse repeatability, while imaging is a secondary one. Equally important, the processing workflow must preserve the 4D signal. Toward this end, each processing step that interacts with seismic amplitude undergoes comprehensive compliance testing to certify that it preserves the 4D signal. Therefore, any processing step that does not

preserve the 4D signal is eliminated from the processing workflow even if it improves the time-lapse repeatability or seismic imaging. To assess the time-lapse repeatability, one needs to use a measure after each processing step. A common method to quantify time-lapse repeatability is to use the normalized root-mean-square (NRMS) diagnostics, which is sensitive to amplitude, time, and phase changes between the baseline and monitor surveys (Kragh and Christie, 2001). A 50 ms time window around the reflector of interest is used to generate the NRMS maps.

During processing, fold, offset, and azimuth ranges are kept unchanged as the acquisition geometry remains constant for all surveys. The prestack processing workflow used for this project is shown in Figure 2. The workflow covers all the processing steps from tape transcription to time migration. The pre-processing includes transcribing the SEGD tape into internal format, uploading the geometry information into trace header, limiting trace length to 1000 samples with a 2 ms sampling rate, applying the elevation statics to bring all sources and receivers to a common seismic reference datum, editing bad traces from all surveys to ensure equal traces for different surveys, and applying t^2 scaling to compensate for the spherical divergence. At the start of the processing, the baseline survey is processed independently to obtain mute and velocity functions needed for stacking. The 3D seismic data for all surveys is, then, sorted and stacked using the velocity and mute functions derived from the baseline survey. To quantify time-lapse repeatability at this stage, an NRMS is computed and recorded.

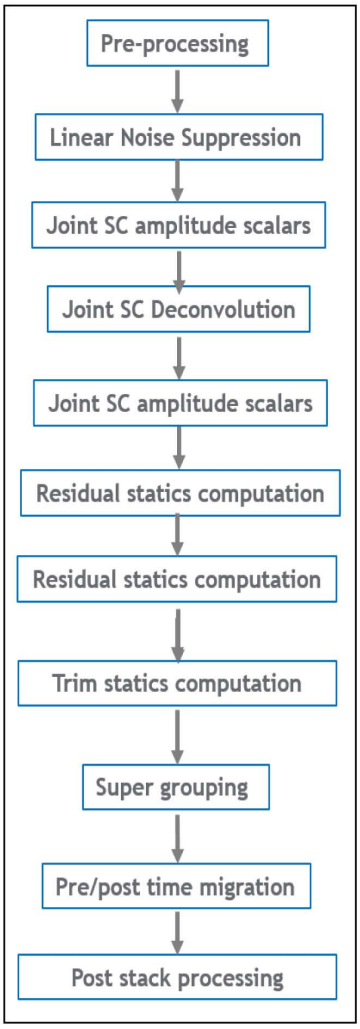

Figure 2—4D processing workflow consists of a combination of simultaneous and joint processing.

A common-receiver gather taken from the baseline survey with applied NMO manifests significant high-amplitude coherent noise that masks the reflected signals as shown in Figure 3 (a). Such linear noise encompasses frequency below 15 Hz. To effectively suppress such coherent noise, a three-step approach is deployed. Initially, the 3D seismic data undergoes a bandpass filter followed by an FK-based technique that is certified as 4D compliant. This is to ensure that the 4D signal is preserved. The last step is to eliminate amplitude bursts on a trace-by-trace basis. The FK-based method is carried out in the common-receiver domain since the wavefield is properly sampled in this domain. The reflected signals are clear after eliminating the high-amplitude coherent noise as shown in Figure 3 (b) for the same receiver gather. A second NRMS map is computed at this stage after applying a non-surface-consistent amplitude scaling for display purposes. Eliminating high-amplitude coherent noise is essential to all subsequent pre-stack processes, such as velocity analysis, residual statics computation, and derivation of amplitude scalars and deconvolution operators.

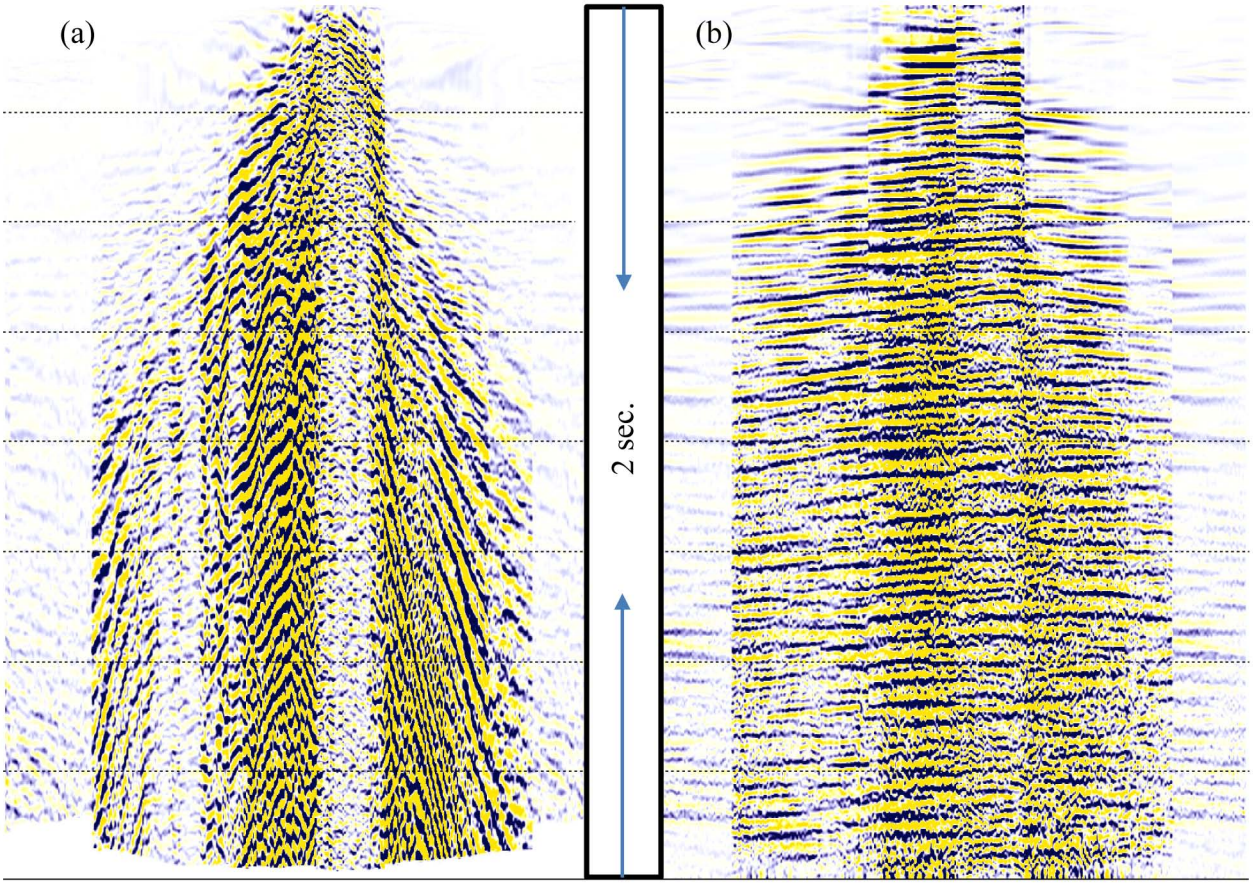

Figure 3—Common-receiver gather showing traces of a single shot line before (a) and after (b) eliminating the high-amplitude coherent noise using a three-step approach. Clearly, the high-amplitude noise is masking the reflected primaries

Variations in source and receiver coupling and near-surface variability may cause amplitude variations of the pre-stack data. These amplitude variations can cover the 4D signal. An innovative joint surface-consistent amplitude-scaling algorithm using four terms (source position, receiver position, offset, and CDP) is exploited to resolve the amplitude variations. The algorithm allows both source and receiver terms to have different scalars for the same positions, but it restricts the other two terms (offset and CDP) to be position-invariant over different 3D seismic surveys, as the window of analysis does not include the reservoir. This is to ensure that the source and receiver terms are survey-specific while the other two terms are survey-independent, thus the amplitude variability are linked to the sources and receivers over space and time. Accordingly, the induced reservoir changes are protected against the overburden changes. The

derived scalars for the sources and receivers of one survey are displayed in Figure 4. The receiver scalars are clustered around value close to one and have a narrow variability unlike the source scalars, which span a wider range of values. The scalars for all terms are applied to each survey independently to ensure that the analysis window has exactly the same amplitude independent of the survey. After applying the amplitude scalars, the NRMS map is computed. Once the amplitude scalars are applied, wavelet shape variations caused by the near-surface layers are addressed by a four-term joint surface-consistent spiking deconvolution algorithm that uses a similar principle as the scaling algorithm, but with a longer analysis window for deriving the deconvolution operators. The deconvolution operators for shots and receivers are applied to remove variations in wavelet shape caused by near-surface variability. Consequently, the wavelet shape remains consistent across all surveys. A second pass of the four-term joint surface-consistent amplitude-scaling algorithm is re-computed to adjust the amplitude changes caused by deconvolution application.

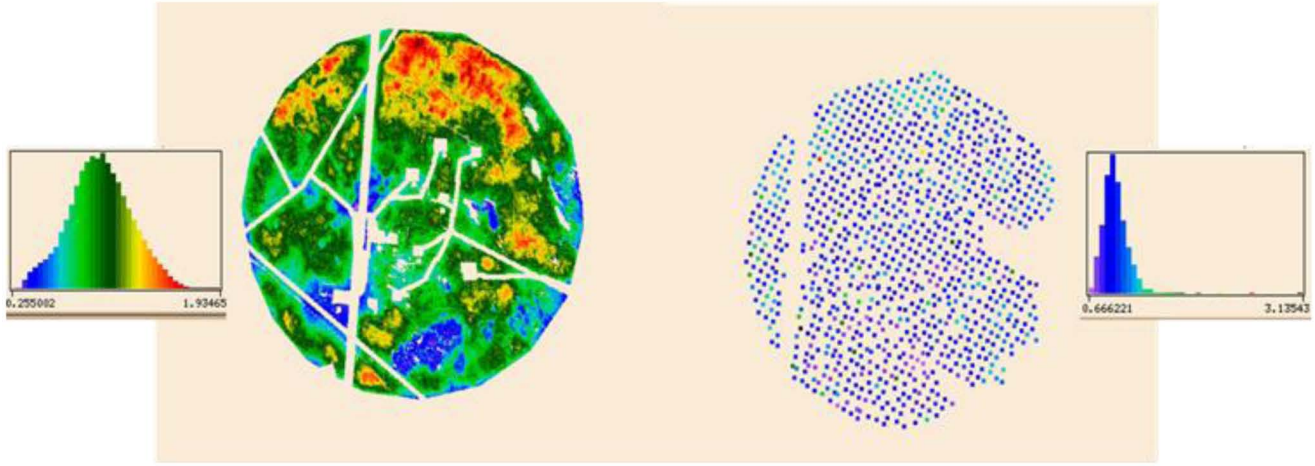

Figure 4—Source scalars for survey 2 are shown to the left of the graph together with their distribution ranging from 0.25 to 2.0; receiver scalars for the same survey are displayed to the right of the graph with their distribution ranging from 0.6 to 1.4, except for three moderately noisy receivers. The map of the receiver scalars is enlarged for display purposes. The actual size of the receiver coverage area with respect to the source coverage area is shown in Figure 1. The scalar values represented with colors accurately follow the variations of the near-surface layer.

The variations in reflection times are resolved by an innovative approach, deploying two passes of a specialized 3D surface-consistent statics algorithm. During the first pass, the variations caused by near-surface variability that is common to all surveys are addressed by using a pilot trace generated from the baseline survey. The algorithm, then, uses the 3D seismic data from the baseline together with the generated pilot trace to calculate the residual statics values. To complete the first pass, the calculated statics values are applied to all surveys independently. This is to ensure that all surveys are aligned with respect to the baseline by removing the effect of the near-surface layer. The rationale behind this step is that the near-surface layer affects all survey in a similar fashion and alignment is preferred for measuring amplitude attributes. During the second pass, the small variations between different surveys (4D statics) caused by seasonal changes, such as temperature, humidity, and sand movements, are computed using a common pilot trace generated from the baseline survey after applying the residual static values calculated in the first pass. Using the updated pilot trace, the 3D surface-consistent residual statics algorithm computes the static values for each survey independently. To complete the second step, the static values, computed during the second pass, are applied to the corresponding surveys. This step is followed by a velocity analysis on the baseline survey to update the velocity functions. This is to ensure that 4D signal is not biased by the velocity analysis. At this point, another NRMS is computed and checked before passing to trim statics.

Trim statics are used to resolve small variations within CDP gathers to enhance the signal-to-noise ratio, align wavelet character, and improve reflector continuity. Though powerful, trim statics may create false structure and mislead interpretation; therefore, one needs to handle trim statics with care. Like residual statics, the pilot trace is constructed using the baseline survey. Using the common pilot trace, the trim statics algorithm calculates the static values for each survey simultaneously. Then the values are applied to their corresponding surveys. At this stage, trim NRMS is calculated and checked before passing to supergrouping. To further enhance the pre-stack data, we apply an innovative supergrouping method that uses 7 by 7 shot groups with NMO applied. This process enhances seismic data by boosting SNR, suppressing random and linear noise, and improving events continuity (Bakulin et al., 2016). The last step in pre-stack processing for improving repeatability is pre-stack/post-stack time migration.

At the end of each processing step, we produce stacks for all surveys and apply a band pass filter, followed by an F-XY deconvolution, before generating NRMS for measuring the 4D noise among such surveys. No cross-equalization was applied in this study due to the very repeatable nature of the data. Figure 5 shows that we have achieved a mean NRMS value of 5.58% for the finale time-lapses processed up to post-stack migration despite all the challenges. This is a major accomplishment in such a harsh environment and it replicates repeatability achieved in marine 4D seismic in areas with much simpler overburdens. The same Figure also highlights that rainy season, ranges from survey 7 to survey 12, create an additional challenges for seismic repeatability. However, the year-to-year repeatability measured over the dry season is close to what was observed within the same season. This highlights cyclic nature of the repeatability in desert environment.

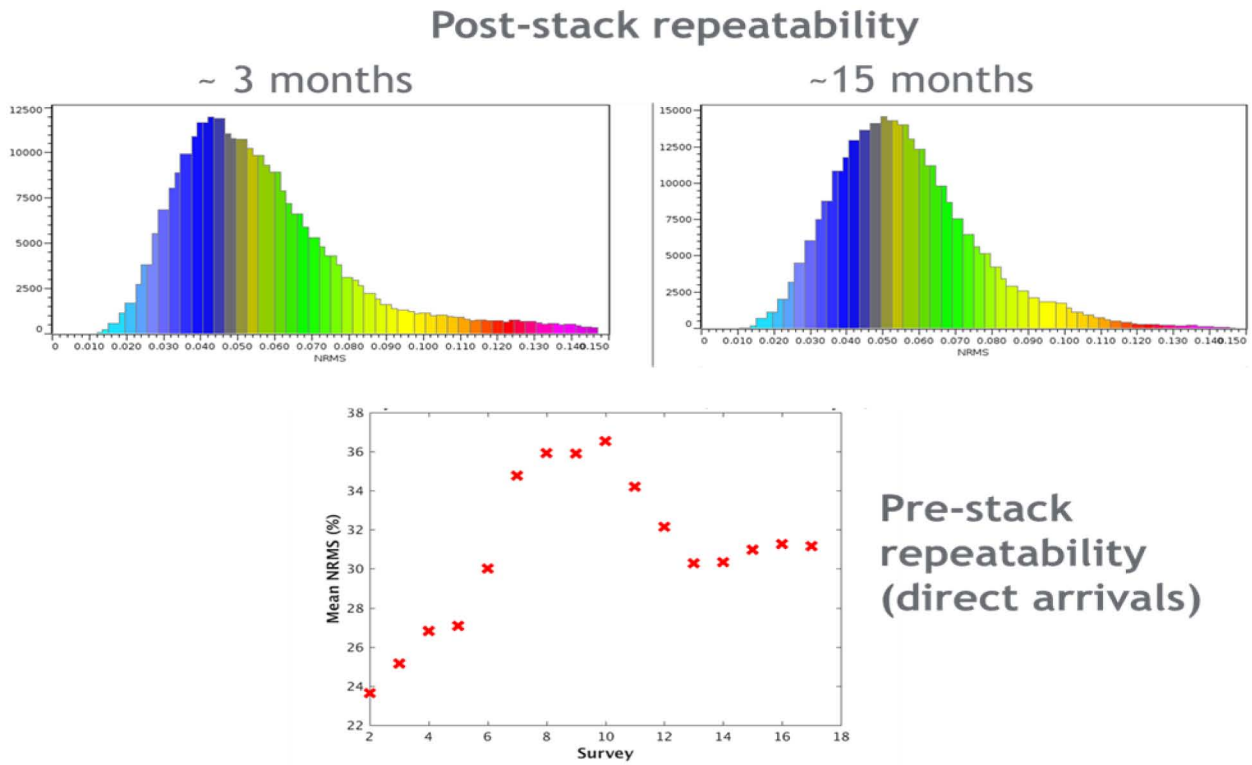

Figure 5—The upper part of the graph shows histograms of post-stack repeatability achieved over 3-month (left) and 15-month (right) periods. Both have mean NRMS of 5.58%. The lower graph shows that pre-stack repeatability is a function of season. Data is more repeatable during the dry season (surveys 1-6, 13-17) than during the rainy season (surveys 6-12) and it also confirms that pre-stack repeatability is cyclic.

Results and discussion

Repeatability between baseline survey and monitor surveys is judged by the NRMS (normalized root-mean-square) metric. NRMS is computed over a given time window (50 ms around the horizon of interest in our case) and ranges from 0%, perfect repeatability, to 200%, the worst case repeatability and indicates that the two volumes have opposite polarity. After pre-processing, we obtain a mean NRMS value of nearly 40%, which is considered quite reseaonable at this stage. Two major factors have led to this low NRMS value. First, the permanent sensors are buried below the weathering layer to avoid 4D noise. Second, applying time-variant scaling to the pre-stack data and stacking high-fold CDP gather improve signal-to-noise ratio considerably. After suppressing the high-amplitude coherent linear noise, we obtain a mean NRMS value of approximately 29%, which is a remarkable reduction from the previous step. Obtaining such an NRMS value suggests that the coherent linear noise is quite unrepeatable. Still, one needs to ensure that the approach used to eliminate such noise does not hurt the 4D signal. Removing the effects of source and receiver coupling and the effect of the near-surface layer on the amplitude has resulted in well-balanced pre-stack data. However, we obtain a mean NRMS value of around 28%, which is extremely close to the step before. This is because the seismic data in the previous step is balanced using time-variant scaling whereas the current step is balanced by surface-consistent amplitude scalars. Therefore, changing the method one uses to balance the seismic data does not seem to reduce the 4D noise significantly. Having said that, the surface-consistent amplitude scaling is essential for 4D-signal detection even if it has not reduced the 4D noise. The surface-consistent deconvolution (SCD) and the second pass of the surface-consistent amplitude scaling (SCA) induce a minor reduction in 4D noise. Most of the wavelet shape variations exist within the overburden. Furthermore, most of such variations occur during the rainy season as shown in Figure 5. Applying residual statics values has induced little or no change in NRMS. At the start of the processing, we derived a set of global residual statics values from the baseline survey using conventional processing and applied such values to all surveys after pre-processing to better suppress the linear noise. Such statics values are kept applied until before the residual statics step. Still, the innovative approach used to compute the residual statics values is essential for uncovering the 4Dsignal. Application of trim statics values has reduced the 4D noise by another 3% on average, which is a comparatively large reduction. Application of supergrouping is another major step in reducing 4D noise and improving repeatability. It has remarkably reduced NRMS down to 10% by increasing signal-to-noise ratio, eliminating random and linear noise, and improving event continuity. Finally, the post-stack migration has further improved repeatability and brought NRMS down to 5.6%. Figure 6 summarizes the progression of mean NRMS throughout the processing flow.

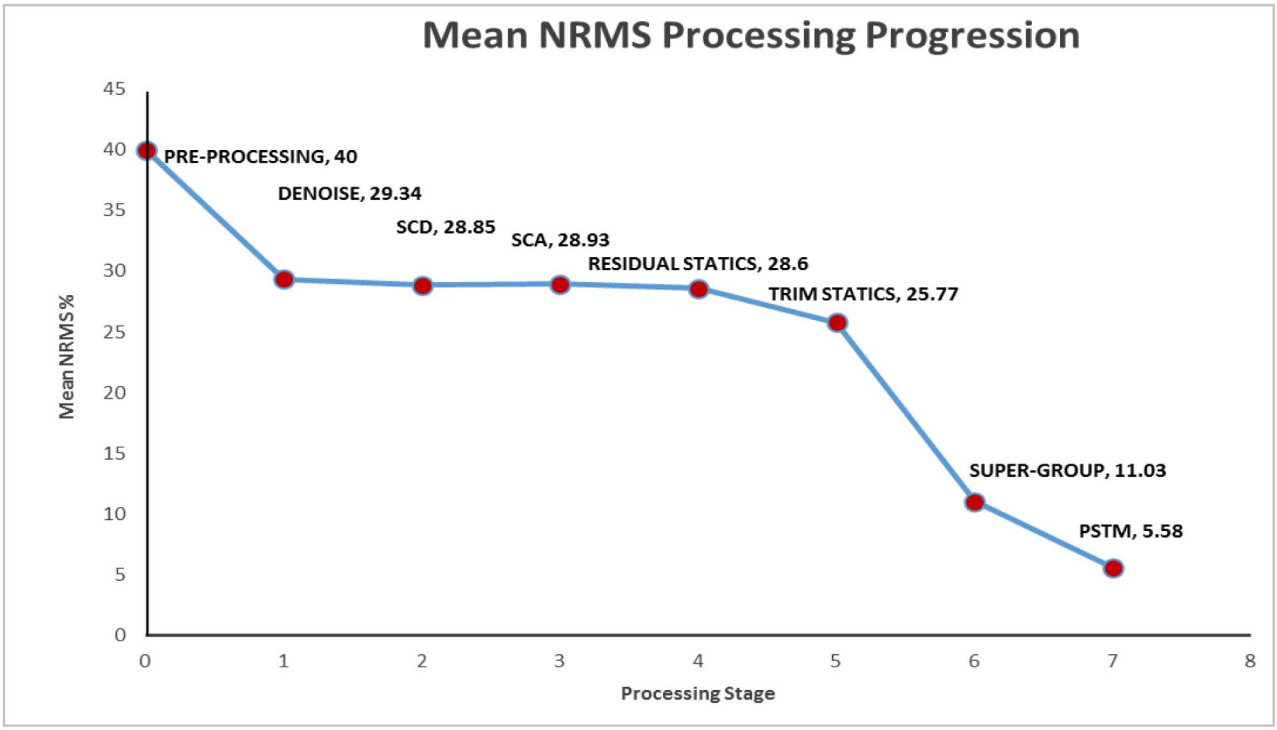

Figure 6—The graph shows progression of mean NRMS of the stacked-data from pre-processing to post-stack time migration. Two processes that have remarkably reduced the mean NRMS value are coherent noise elimination and supergrouping. The surface-consistent processing including SCD, SCA and residual statics have been essential for 4D signal detection.

Conclusions

We have presented a novel 4D processing workflow for 3D surface source/buried receiver data that was continuously acquired to monitor CO2 injection into a stiff carbonate reservoir in Eastern Province of Saudi Arabia. The success of such a processing workflow relies on reducing the 4D noise below the 4D signal level in a harsh arid environment with a challenging near-surface environment. Ultimately, the combination of buried receivers, carpet shooting, and novel processing has delivered seismic repeatability of around 6% NRMS, which is an excellent result and matches the repeatability achieved in marine 4D seismic. While surveys within the wet season exhibit deterioration in repeatability (high NRMS values), repeatability returns to the previous lower levels, when the dry season returns. This is a first of its kind single-sensor permanent monitoring system combined with an innovative processing workflow. Multi-survey surface-consistent processing, supergrouping, and 4D-compliant statics were key steps to obtain repeatable images from these challenging data. This study confirms that onshore 4D noise can be effectively tackled with buried receivers and innovative processing. As a result, we are able to observe some reservoir variations related to CO_2 injection into stiff carbonate reservoir.

Acknowledgements

We would like to express our appreciations to Saudi Aramco for providing us with continuous support and for allowing us to publish this work.

References

Arts, R. J., X. Zhang, A. R. Vedel, D. Sanotonmico, J. A. C. Meekes, R. P. Noorlandt, D. F. Paap, and V. P. Vandweijer, 2013, Experiences with a permanently installed seismic monitoring array at the CO_2 storage sit at Ketzin (Germany) – A status overview: *Energy Procedia*, **37**, 4015-4023.

Bakulin, A., Burnstad, R., Jervis, M. and Kelamis P., 2012. Evaluating Permanent Seismic Monitoring with Shallow Buried Sensors in a Desert Environment. SEG 82nd Annual Meeting, Las Vegas. 1-5.

Bakulin, A., J. Lopez, I. S. Herhold, and A. Mateeva, 2007, Onshore monitoring with virtual-source seismics in horizontal wells: Challenges and solutions: 77th Annual International Meeting, SEG, Expanded Abstracts, 2983-2897.

Bakulin, A., Smith, R., Jervis, M., Saragiotis, C., Al-Hemyari, E. and Alramadhan, A., 2016. Processing and Repeatability of 4D Buried Receiver Data in a Desert Environment. SEG 86th Annual Meeting, Dallas. 5405-5409.

Fanchi, J. R., Pagano, T. A. and Davis, T. L., 1999. State of the Art of 4D Seismic Monitoring: The Technique, the Record, and the Future. *Oil&Gas Journal.* **97** (22).

Han, D. H. and M. Batzle, 2000. Velocity, Density and Modulus of Hydrocarbon Fluids – Data Measurement. SEG 70th Annual Meeting, Calgary. 1862-1876.

Ivandic, M., C. Yang, S. Lüth, C. Cosma, and C. Juhlin, 2012, Time-lapse analysis of sparse 3D seismic data from the CO_2 storage pilot site and Ketzin, Germany: *Journal of Applied Geophysics*, **84**, 14-28.

Ivanova, A., A. Kashubin, N. Juhojuntti, J. Kummerow, J. Henninges, S. Lüth, and M. Ivandic, 2012, Monitoring and volumetric estimation of injected CO_2 using 4D seismic, petrophysical data, core measurements, and well logging: A case study at Ketzin, Germany: *Geophysical Prospecting*, **60**, 957-973.

Kragh, E. and Christie, P., 2001. Seismic Repeatability Normalized RMS and Predictability. SEG 71st Annual Meeting, San Antonio. 1656-1659.

Li, X., R. Couzens, J. P. Grossman, and K. Lazorko, 2012, Simultaneous time-lapse processing for improved repeatability: *First Break*, **30**, 107-110.

Lumley, D. E., 2001, Time-Lapse seismic reservoir monitoring: *Geophysics*, **66**, 50-53.

Lumley, D. E., 2010, 4D seismic monitoring of CO_2 sequestration: *The Leading*, **29**, 150-155.

Lumley, D. E., D. C. Adams, M. A. Meadows, and S. P. Cole, 2003, 4D seismic data processing issues and examples: 73rd Annual International Meeting, SEG, Expanded Abstracts, 1394-1397.

Kragh, E. and Christie, P., 2001. Seismic Repeatability Normalized RMS and Predictability. SEG 71st Annual Meeting, San Antonio. 1656-1659.

Ma, J., L. Gao, and I. Morozov, 2009, Time-lapse repeatability in 3C-3D dataset from Weyburn. CO2 sequestration project: CSPG CSEG CWLS Convention, Expanded Abstracts, 255-258.

Meadows, M. A. and S. P. Cole, 2013, 4D seismic modeling and CO2 pressure-saturation inversion as the Weyburn Field, Saskatchewan: *International Journal of Greenhouse Gas Control*, **16**, S103-S117.

Meunier, J., F. Huguet, and P. Meynier, 2001, Reservoir monitoring using permanent sources and vertical receiver antennae: *The Cere-la-Ronde case study: The Leading Edge*, **20**, 622-629.

Pevzner, R., V. Shulakova, A. Kepic, and M. Urosevic, 2011, Repeatability analysis of land time-lapse seismic data: CO_2CRC Otway pilot project case study: *Geophysical Prospecting*, **59**, 66-77.

Rickett, J.E., and D. E. Lumley, 2001, Cross-equalization data processing for time-lapse seismic reservoir monitoring: A case study from the Gulf of Mexico: *Geophysics*, **66**, 1015-1025.

Roach, L. A. N., D. J. White, and B. Roberts, 2015, Assessment of 4D seismic repeatability and CO2 limits using a sparse permanent array at the Aquistore CO2 storage site: *Geophysics*, **80**, 2, WA1-WA13.

Schisselé, E., E. Forgues, J. Echappé, J. Meunir, O. De Pellegars, and C. Hubams, 2009, Seismic repeatability: Is there a limit?: 9th Middle East Geoscience Conference and Exhibition, Expanded Abstracts, 21.

Trop, T. A., and J. Gale, 2004, Demonstrating storage of CO_2 in geological reservoirs: The Sleipner and SACS projects: *Energy Procedia*, **29**, 1361-1369.

Urosevic, M., R. Pevzner, A. Kepic, P. Wisman, V. Shulakova, and S. Sharma, 2010, Time-lapse seismic monitoring of CO_2 injecting into a depleted gas reservoir – Naylor Field, Australia: *The Leading Edge*, **29**, 164-169.

White, D. J., L. A. N. Roach, and B. Roberts, 2014, Time-lapse seismic performance of a sparse permanent array: Experience from the Aquistore CO_2 storage site: *Geophysics*, **80**, 2.